ANNUAL REVIEWS

Annual Review of Earth and Planetary Sciences

Mimas: Frozen Fragment, Ring Relic, or Emerging Ocean World?

Alyssa Rose Rhoden

Southwest Research Institute, Boulder, Colorado, USA; email: Alyssa@boulder.swri.edu

Annu. Rev. Earth Planet. Sci. 2023. 51:367–87

The *Annual Review of Earth and Planetary Sciences* is online at earth.annualreviews.org

https://doi.org/10.1146/annurev-earth-031621-061221

Keywords

ocean worlds, tectonics, rotational dynamics, satellite formation

Abstract

Mimas, the smallest and innermost of Saturn's mid-sized moons, has a heavily cratered surface devoid of the intricate fracture systems of its neighbor, Enceladus. However, Cassini measurements identified a signature of an ocean under Mimas' ice shell, although a frozen ice shell over a rocky interior could not be ruled out. The Mimas ocean hypothesis has stimulated inquiry into Mimas' geologic history and orbital evolution. Here, we summarize the results of these investigations, which (perhaps surprisingly) are consistent with an ocean-bearing Mimas as long as it is geologically young. In that case, a ring origin for Mimas is favored over primordial accretion. An independently developed model for the formation of a gap in Saturn's rings provides a potential mechanism for generating a late-stage ocean within Mimas and may have assisted in the development of Enceladus' ocean and associated geologic activity. Rather than a battered relic, Mimas may be the youngest ocean moon in the Saturn system, destined to join Enceladus as an active world in the future. The presence of oceans within Saturn's mid-sized moons also has implications for the habitability of Uranus' moons; the Uranus system was chosen as the highest priority target for the next NASA Flagship-class mission.

- Models of Mimas' tides and rotation state support a present-day internal ocean.
- Mimas' craters, impact basin, and lack of widespread tectonism are compatible with a stable/warming ocean.
- The formation of the Cassini Division within Saturn's rings provides a potential pathway to a present-day ocean within Mimas.
- If Mimas has an ocean today, it is geologically young.

1. INTRODUCTION

The satellite systems of our two gas giant planets, Jupiter and Saturn, display very different manifestations of the processes that govern satellite formation and evolution (**Figure 1**, in which all bodies are scaled to the same planet size). At Jupiter, we find four large moons that decrease in density and geologic activity with distance from Jupiter (e.g., Matson et al. 2009, Hussmann et al. 2015); these differences can be linked to the abundance of radiogenic material to heat each moon's interior and the availability of tidal heating. At Saturn, we find a very different satellite system (**Figure 1**). While the total mass of the satellites in each system is similar, relative to the masses of their parent planets, that mass is distributed across many more moons at Saturn than at Jupiter. Only one moon, Titan, is comparable in size to the regular satellites of Jupiter. Titan orbits at a distance of 20 Saturn radii (R_S), which is comparable in distance to Ganymede and Callisto. There are also five smaller moons interior to Titan. The mid-sized icy moons—Mimas, Enceladus, Tethys, Dione, and Rhea—all orbit closer to Saturn than Europa orbits Jupiter and are all less than half the size of Europa, creating a packed inner satellite system.

The mid-sized moons display the full spectrum of compositional makeup, geologic activity, and thermal evolution observed at Jupiter, but the connection between distance and the characteristics of the moons is quite different (for a review, see Castillo-Rogez et al. 2018). The mid-sized moons increase in mass and radius with distance from Saturn, but not in density. The mid-sized moon with the lowest rock content is Tethys (third from Saturn), followed by the innermost moon, Mimas. Orbiting in between these two moons is Enceladus, which has the highest density of the mid-sized moons. Hence, the compositional gradient observed at Jupiter is not replicated at Saturn. The

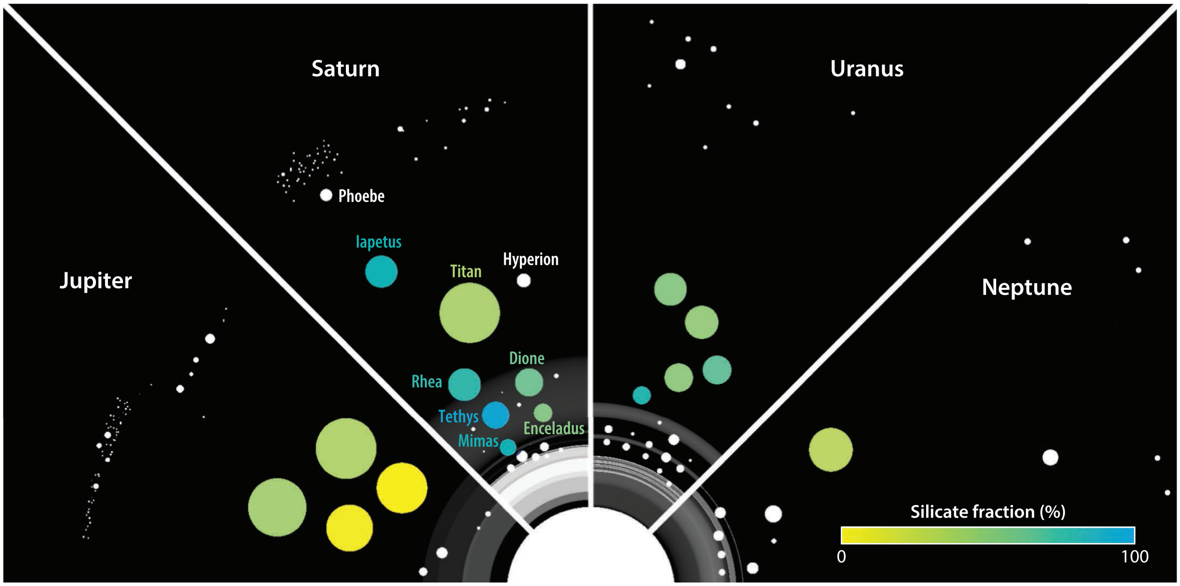

Figure 1

The satellite systems of the four giant planets in our Solar System, shown here scaled to a consistent planet size, display a great deal of diversity. At Jupiter, there are diffuse rings and four large moons that decrease in density geologic activity with distance. In contrast, Saturn and Uranus each have dense rings and a suite of mid-sized moons with compositions and levels of activity that are not tied to their locations. By comparing these systems, we can explore how such diversity occurred, constrain the likely thermal evolutions of the moons, and assess the likelihood of forming oceans within mid-sized icy worlds. Figure adapted from NASEM (2022).

two moons with highest density, Enceladus and Dione, display the most geologic activity, as described below, but the other three moons show no clear correlation between density and geologic activity.

In terms of geology, Enceladus generally steals the show, with its active geysers and extensive (young) fracture systems (Porco et al. 2006). Dione has multiple classes of fractures, including the unique wispy terrain, which Cassini revealed to be bright fractures and parallel fracture sets (Collins et al. 2009). Rhea is heavily cratered with some evidence of past tectonic activity. Tethys possesses a global-scale canyon system, Ithaca Chasma, along with grooves of uncertain origin. Mimas is heavily cratered, with no canyons or widespread tectonics. Only about a dozen fractures have been identified, globally (Schenk et al. 2018). (For a more detailed overview of the geology of the mid-sized moons, see Collins et al. 2009 or Schenk et al. 2018, and references therein.)

The extent of geologic activity on the mid-sized moons is correlated with the magnitude of inferred heat flow over time. The active south polar region of Enceladus has incredibly high heat flows (Spencer et al. 2006), and even craters well outside the south pole record an epoch of high heat flows (Bland et al. 2012). Craters on Tethys, Dione, and Rhea have also been modified over time by relatively high heat flows from the interior (White et al. 2013, 2017), despite these moons having limited sources of heat in the present day (Castillo-Rogez et al. 2018). Mimas' craters show no evidence of such modification from heating (Schenk 1989, Schenk et al. 2018), although the combination of limited topographic resolution at Mimas and Mimas' very low gravity would make it difficult to identify. Again, the gradient of geologic activity with distance that we observe among Jupiter's moons is absent at Saturn.

Overall, Mimas seems like the least interesting of Saturn's mid-sized moons due to its small size, lack of geologic activity, and little evidence of a history of internal heating, which is surprising when considered through the lens of the Jovian moons. Mimas orbits substantially closer to Saturn than Io does to Jupiter, and it has a higher eccentricity that ought to promote significant tidal heating. However, Mimas does not display any substantial tectonic or volcanic activity (e.g., Schenk et al. 2018). The lack of geologic evidence of tidal heating implies that Mimas has been cold since it last assembled, such that it has remained fairly unresponsive to tides (e.g., Matson et al. 2009, Castillo-Rogez et al. 2018). The present-day high eccentricity also suggests a cold history for Mimas because otherwise tidal dissipation should have acted to rapidly circularize Mimas' orbit, particularly in the absence of a mean motion resonance that could force the eccentricity to remain high (e.g., Peale 1999). Given Mimas' low density and inferred low rock fraction, it is reasonable to expect limited heating from radiogenic material, and its small size would limit initial accretion heating and allow Mimas to cool fairly rapidly (Matson et al. 2009, Hussmann et al. 2015, Castillo-Rogez et al. 2018). Hence, the differences between active Io and inactive Mimas can be explained by differences in their size and composition, which controlled the availability of internal heat sources and kept Mimas from experiencing runaway tidal heating. Unfortunately, Cassini observations of Mimas' rotational librations rule out this simple history.

Mimas has large librations, which are inconsistent with an undifferentiated body. Model fits to the Cassini data show that Mimas must have either an elongated core under a frozen shell or a spherical core, a liquid water ocean, and an ice shell 24–31 km thick (Tajeddine et al. 2014), as illustrated in **Figure 2**. Additional modeling of the libration phase supports the ocean interpretation (Noyelles 2017) and shows that the core may be elongated even in the presence of an ocean (Caudal 2017). Whether or not there is an ocean within Mimas, the librations complicate our picture of Mimas' evolution because it must have either formed layered, which is not a natural outcome of standard accretion formation, or heated up sufficiently to differentiate, despite having limited heat sources. Proposed models for Mimas' formation, and their implications on its thermal history, are described in Section 2.

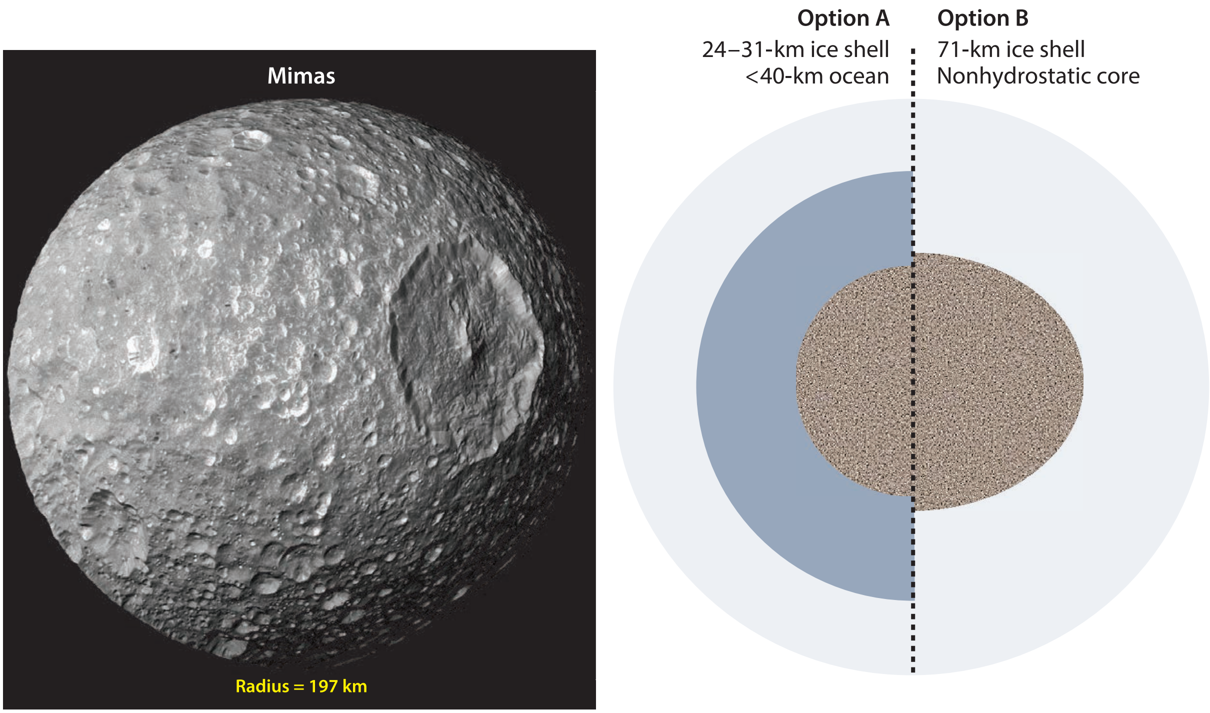

Figure 2

Mimas' heavily cratered surface suggests it is a frozen world that never experienced significant warming, dissipation, or geologic activity. However, Mimas' measured librations indicate that its interior must be separated into a rocky interior and icy exterior (Tajeddine et al. 2014). Adding a global, liquid water ocean below the ice improves the match to the phase of Mimas' librations, forcing us to reconsider the interpretation of Mimas as a geologically inert world. In the ocean model, the ice shell must be 24–31 km thick, which could induce considerable tidal heating and stress. The constraints on Mimas' interior structure in the presence of an ocean can, thus, be used to determine whether tidal heating could sustain the inferred ocean-ice shell configuration. If not, the Mimas ocean hypothesis can be safely ruled out. Photo PIA 12570, courtesy of NASA/JPL-Caltech/Space Science Institute.

There are also several geologic barriers to Mimas being a present-day ocean world, as described in detail in Section 3. Specifically, an ocean-bearing Mimas must be able to retain a thick ice shell in the presence of high tidal heating in order to match the libration constraints (Tajeddine et al. 2014), produce limited thermal modification of craters over the surface age, and produce limited tectonic activity despite high tidal stress. There may also be limits on the longevity and thermal evolution of the ocean, provided by the Herschel impact basin. Either the present-day ice shell was able to survive the Herschel-forming impact or the shell has thinned since the impact occurred. Finally, we must consider Mimas in context with its neighbors: Saturn's rings (interior) and Enceladus (exterior). The rings are massive and close enough to Mimas that the gravitational interactions between them can be significant (e.g., Colwell et al. 2009). Hence, the history of the rings can help bound Mimas' recent orbital evolution, which drives the engine of tides within Mimas. Comparing the inferred thermal histories of Mimas and Enceladus may provide additional clues as to their origins and common processes.

Here, we evaluate each of the observational constraints on Mimas' interior to determine the conditions under which the geologic record would be compatible with a present-day ocean. The investigations we describe show that Mimas' geology is consistent with a young ocean that has been developing at least since the formation of the Herschel impact basin. Constraints on Mimas' recent thermal-orbital evolution, identified from the architecture of Saturn's rings, provide a pathway for forming a late-stage ocean within Mimas. In comparison with Enceladus, it is plausible that Mimas is at an earlier stage of a similar evolutionary process and may be transitioning to a state of higher geologic activity, more similar to Enceladus. Although more modeling is needed to connect the recent histories of these moons with their origins, the scenario in which the mid-sized moons are born from Saturn's rings seems most consistent with an initial unheated, layered structure and the core properties needed to achieve high tidal dissipation observed at Enceladus.

If Mimas is ocean bearing, it provides additional constraints on the conditions under which mid-sized, icy moons can generate oceans, with implications for the habitability of the Saturn system. Furthermore, the ocean must be geologically young, presenting an opportunity to explore the early epoch of ocean moon evolution. Finally, the Uranus system also possesses rings and mid-sized icy moons with diverse records of geologic activity (e.g., Collins et al. 2009). By understanding the formation, evolution, and habitability of the Saturn system, we prepare for future exploration of the Uranian system. Even if Mimas does not have an ocean today, the fact that its evolution does not conform to our expectations provides the motivation to explore new mechanisms by which icy moons can form and further investigate what controls the diversity of moons across different giant planet systems.

2. HYPOTHESES OF MIMAS' FORMATION

There are currently multiple hypotheses for the formation of Mimas and the other mid-sized icy moons of Saturn, which can affect the thermal evolution of their interiors. The original hypothesis was that Mimas formed billions of years ago within a circumplanetary disk (CPD) around Saturn (e.g., Canup & Ward 2006). Neveu & Rhoden (2017) modeled the thermal-orbital evolution of a primordial Mimas under several scenarios. They found that it is challenging to heat Mimas to the point of differentiation without an additional source of heat beyond their canonical case (e.g., very early accretion to retain more radiogenic heating or artificially enhanced tidal dissipation). If the perhaps unrealistic conditions necessary to kick off differentiation are imposed, tidal dissipation rapidly circularizes Mimas' orbit, leading to a negligible present-day eccentricity and a semi-major axis beyond the present-day orbit of Enceladus. Mimas can then freeze, matching the layered structure implied by the libration measurement, but additional mechanisms are required to modify the orbit to match the observed orbital distance and eccentricity (Neveu & Rhoden 2017).

There are also formation models in which Mimas and Enceladus (and perhaps other mid-sized moons) reassembled from debris produced in massive collisions of precursor moons (e.g., Asphaug & Reufer 2013, Ćuk et al. 2016). Disruptive impacts are certainly plausible, particularly for smaller moons that formed early in Solar System history (e.g., Nimmo & Korycansky 2012, Movshovitz et al. 2015). The interior structure of a reassembled moon and its ability to generate an internal ocean are not well understood and likely depend on the preimpact differentiation state of the disrupted moon, the compositions of the moon and impactor, the energetics of the collision, and the manner of its reassembly. For example, Movshovitz et al. (2015) predicted that a reassembled Mimas should be undifferentiated and homogeneous, based on their collisional models, a scenario that is now ruled out by the libration measurements.

In contrast, Dubinski (2019) posited that partial disruption of a differentiated progenitor moon, with twice the mass of Mimas, could have resulted in a layered Mimas while simultaneously creating Saturn's icy rings. However, this model requires a differentiated progenitor, orbiting even closer to Saturn than present-day Mimas, that avoids disruption until very recently in Solar System history. Finally, Asphaug & Reufer (2013) suggest that Mimas and the other mid-sized icy moons were formed from chuncks of ejecta after the disruption of a proto-Titan, with the density variations representing the amount of mantle material exhumed in the impact. The thermal evolution of the interiors of the fragments has not yet been modeled. Clearly, more studies are needed to determine the suite of conditions that can produce a layered Mimas, whether ocean bearing or frozen, after disruptive impacts into preexisting moons.

Alternatively, it has been suggested that both Mimas and Enceladus initially formed in Saturn's rings. Viscous spreading of the rings can bring material through Saturn's Roche limit, allowing the material to accumulate into a moon before migrating outward through a combination of ring and tidal torques (Charnoz et al. 2011, Salmon & Canup 2017). A compelling component of ring formation is that the observed increase in the mass and radius of the mid-sized moons with distance from Saturn is a natural outcome of the model (Charnoz et al. 2011, Salmon & Canup 2017). The ring formation model by Charnoz et al. (2011) assumes that an initial rocky ring particle accretes ice as it moves outward, forming a mid-sized moon. This mechanism naturally results in a layered structure that is compatible with the libration measurements without requiring heating within Mimas. In Salmon & Canup (2017), Mimas accretes from icy ring particles, and the rocky component is delivered later, by impacts, with differentiation driven by impact heating. In this model, Mimas does not have to experience global-scale internal melting to differentiate, which may allow it to retain its eccentricity and avoid extensive tidal heating. However, the tidal heating that could be produced during impact-induced differentiation has yet to be studied, so the model cannot be fully vetted against Mimas' present-day eccentricity. Regardless of which way Mimas formed, once assembled and layered, an additional mechanism would be required to transition a frozen Mimas to a present-day ocean world, as none of these formation models have been shown to produce an ocean in Mimas.

An implication of a ring formation model is that the mid-sized moons (from Mimas to Rhea) would have different ages, by perhaps of order a billion years, depending on model parameters (e.g., Charnoz et al. 2011). In contrast, primordial formation would imply ages of billions of years. Crater densities are often used to date planetary surfaces, but there are significant challenges in such analyses at Saturn. A critical component of age dating using craters is knowledge of the size frequency distribution (SFD) of impactors. In the inner Solar System, detailed observations of the asteroid belt, along with radiometrically dated lunar samples, provide the necessary information to constrain surface ages with crater densities (e.g., Neukum et al. 2001, Hiesinger et al. 2012, Bottke et al. 2015). However, the outer Solar System is subjected to a completely different impactor population, much of which is derived from the primordial Kuiper Belt. Exploration of the Pluto-Charon system by the New Horizons spacecraft improved our knowledge of the historical impactor flux within the Kuiper Belt (Greenstreet et al. 2015, Singer et al. 2019), which is fairly well represented by a hypothetical estimate of the impactor flux known as Case A (Zahnle et al. 2003). Unfortunately, the crater distributions on Saturn's moons are not well matched by the Case A population and display many more small-scale craters than are observed on Charon (Kirchoff et al. 2018; Ferguson et al. 2020, 2022a,b), implying that the moons of Saturn have been subjected to a population of planetocentric (Saturn-orbiting) impacts, for which the SFD of impacting material is unknown. Until the sources and timescales for the delivery of planetocentric material at Saturn can be constrained, the diagnostic value of craters for dating the moons is limited.

3. OBSERVATIONAL CONSTRAINTS ON MIMAS' HISTORY

3.1. The Effects of Tides on the Geology of an Ocean-Bearing Mimas

3.1.1. A brief overview of tides in icy moons. The gravitational pull of a planet on its moon will act to deform the global shape of the moon such that it becomes elongated in the direction of the planet, through the process of tides (e.g., Peale 1999, Schubert et al. 2010). If the moon is in a circular orbit and synchronous rotation (i.e., the spin rate is the same as the orbital rate, so the same point on the moon faces the planet at all times), the tidally distorted shape of the moon becomes permanent, and any stress caused by the initial deformation relaxes away. This shape is referred to as the primary tidal shape. However, if the moon is in an eccentric orbit, the distance between the moon and the planet will change throughout an orbit, as will the direction to the planet from the reference frame of the moon. In this case, there is an additional, periodic tidal deformation acting on the primary tidal shape caused by the moon trying to match a tidal configuration that is constantly changing (e.g., Greenberg et al. 1998). These deformations can occur quickly enough to induce tidal stress in the moon, and friction produced by the global shape changes can induce tidal heating (e.g., Peale et al. 1979). Over time, tidal dissipation and additional gravitational interactions between the planet and moon will act to decrease the eccentricity and circularize the orbit. However, if the moon is in a mean motion resonance with another moon in the system, the eccentricity can be maintained even in the presence of tidal dissipation. It is this mechanism that has kept the eccentricities of Io and Europa high despite their intense tidal activity (Greenberg et al. 1998, Peale 1999, Hussmann et al. 2015).

Generally, the amount of tidal stress and tidal heating increases with eccentricity and proximity to the planet, but the extent to which the interior can respond to tidal forcing is a determining factor. In ocean moons such as Europa, the ice shell is mechanically decoupled from the interior by the underlying ocean, allowing the outer layers to more freely respond to tidal forcing (e.g., Jara-Orué & Vermeersen 2011, Hussmann et al. 2015). The ocean can rapidly respond to the changing tides, just as Earth's oceans respond to lunar tides, imposing stress on the overlying, less-deformable ice shell. The amount of tidal heating generated in a moon will depend on the orbital frequency that drives the deformation. Each frequency will preferentially deposit tidal heat in material of a specific viscosity. For close-in moons of giant planets, which typically have orbital periods of a few days or less, tidal heat is concentrated in the warm ice layers near the ice-ocean interface (e.g., Walker & Rhoden 2022). If the moon is entirely frozen, the ice at the base of the shell is not warm enough to dissipate. Hence, the presence of an ocean causes a substantial change in the responsiveness of a moon's outer layers to tidal deformation and can vastly increase the tidal stress and tidal heating, depending on the orbit of the moon.

To reproduce Enceladus' extensive heat flows, it has been proposed that the properties of the cores of ice-rich moons may also provide significant heat. If a moon's core is a porous aggregate of rock and ice (termed fluffy), the core itself can be responsive to tidal forcing, generating considerably more heat than compact, silicate cores (Roberts 2015, Choblet et al. 2017, Liao et al. 2020, Rovira-Navarro et al. 2022). Currently unknown is how such a core could remain fluffy through the formation, and presumed differentiation, of Enceladus and whether Mimas and the other mid-sized icy moons also possess fluffy cores.

3.1.2. Tidal heating, ice shell thickness, and Mimas' limited crater relaxation. Given its high eccentricity of ~0.02 (four times that of Enceladus) and close proximity to Saturn (~3 R_S), tidal heating in an ocean-bearing Mimas could be extensive, particularly if it has a warm, thick ice shell. Mimas may, thus, produce too much heat to maintain the relatively thick ice shell (24–31 km) required to match the libration measurements (Tajeddine et al. 2014). In the presence of an ocean, the temperature at the base of the shell would be fixed at or near 270 K while the surface is 60–90 K (Howett, et al. 2011, Rhoden & Walker 2022). The viscosity of the warm ice near the base of the ice shell makes it highly dissipative when forced at Mimas' mean motion period of 23 h. If the ice shell is too thick, it will produce more tidal heating than it can transport out of the shell, leading it to melt back to a thermally stable thickness. Likewise, if the ice shell were too thin, there would not be a large enough volume of material in which to generate tidal heat, and the ice shell would thicken. Thus, assessing the tidal heating generated within Mimas' ice shell can provide a constraint on the range of plausible ice shell thicknesses and test the ocean hypothesis.

Rhoden & Walker (2022) computed tidal heating and surface heat flow for an ocean-bearing Mimas for a suite of possible parameters to determine the range of stable ice shell thicknesses using Mimas' present orbital distance, eccentricity, and librations. They applied an Andrade rheology model to the ice shell, which has been shown to better mimic the behavior of ice under the forcing conditions of close-in moons than the typical Maxwell model (e.g., Castillo-Rogez et al. 2011). In addition to tidal heating, the amount of heat flowing into the ice shell from below (i.e., the basal heat flux) will contribute to the overall amount of heat that must be transported out of the shell to achieve thermal stability. Because the basal heat flux from Mimas' interior is not well constrained, Rhoden & Walker (2022) selected a suite of ice shell thicknesses, computed tidal heating generated within the shell, modeled the transport of heat out of the shell, and then identified the basal heat required to achieve thermal equilibrium for each thickness.

As shown in **Figure 3**, sustaining very thin ice shells (e.g., <5 km) would require high basal heat fluxes (of order 100 mW/m^2), which are highly unlikely given Mimas' low rock fraction and resulting low radiogenic heating (e.g., Matson et al. 2009). Furthermore, such thin shells are ruled out by the observed geology, including the depth of the Herschel impact basin (∼10 km) (Schenk et al. 2018). On the other end of the spectrum, ice shells thicker than 29 km cannot be thermally stable because they produce too much heat even with minimal basal heating (Rhoden & Walker 2022) (**Figure 3**). Hence, at the present-day eccentricity, an ice shell thicker than 29 km

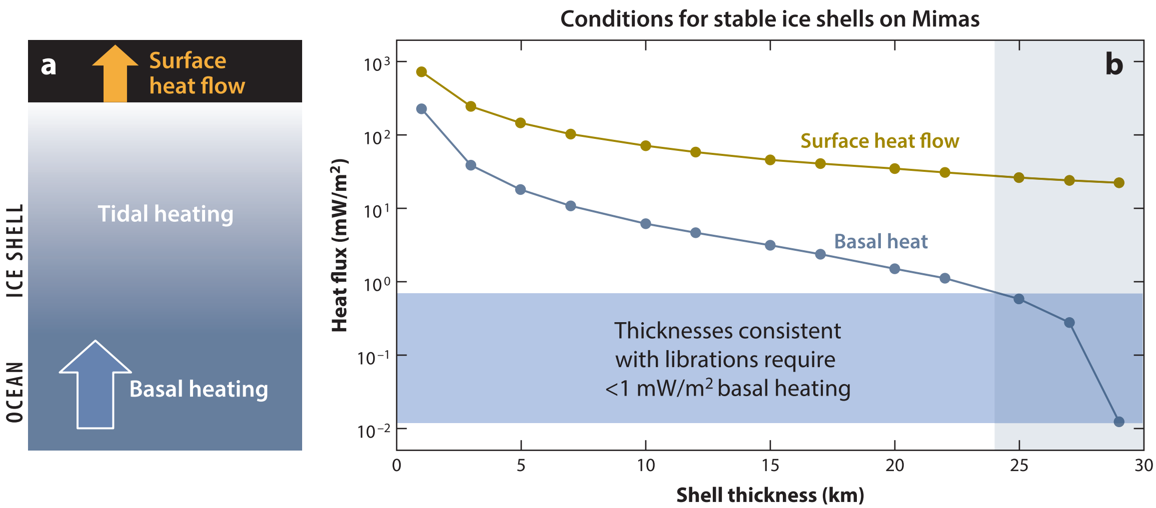

Figure 3

With Mimas' current eccentricity, semi-major axis, and inferred subsurface ocean, tidal heating will be generated within its ice shell. Basal heating from the interior can also enter the shell from below, although the expected contribution to the overall heat budget is small (e.g., Matson et al. 2009). In order for an ice shell to be thermally stable, it must be able to transport heat from the interior to the surface, resulting in the surface heat flow. This system is illustrated in panel *a*. Panel *b* shows the amount of basal heat (*blue symbols*) required to maintain an ice shell of a specific thickness (*x* axis). Thick shells produce large amounts of tidal heating, so the basal heat requirement is low, whereas thin shells have less material in which to dissipate, requiring higher basal heat fluxes to achieve stability. Ice shells thicker than 29 km are never stable at Mimas' current conditions. They would be in a state of melting in response to the high tidal heat production. Ice shells between 24 and 29 km, which are within the range indicated by Mimas' librations (*shaded region*) (Tajeddine et al. 2014) are stable with minimal heating from below. The surface heat flow (*orange symbols*) is very sensitive to the ice shell thickness, as the thickness sets the amount of tidal heating. Measurements of surface heat flow may, thus, be used to test the Mimas ocean hypothesis and, potentially, constrain the ice shell thickness. Figure adapted from Rhoden & Walker (2022).

would be actively melting. Interestingly, for the low basal heat fluxes expected for Mimas (<1 to ~10 mW/m^2), the thermally stable ice shell thicknesses fall between 24 and 29 km, which overlaps with the range of thicknesses indicated by Mimas' librations. In other words, tidal heating in an ocean-bearing Mimas would sustain an ice shell of the correct thickness to match the libration results using the most realistic parameters.

Because thermally stable ice shells must be able to transport out all of the tidal and basal heating within the ice shell, it is possible to calculate the surface heat flux associated with a particular shell thickness. As shown in **Figure 3** (modified from Rhoden & Walker 2022), for ice shells 24–29 km thick, the surface heat flow would be 21–28 mW/m^2, which may affect the topography of surface features over time. For example, heat flow through ice shells causes craters to slowly change shape through a process called relaxation (e.g., Dombard & McKinnon 2006). For the same size crater, a shallower depth is taken as an indication of relaxation (Dombard & McKinnon 2006), particularly in the absence of other types of morphological changes, such as wall slumping or (at Enceladus) infill by plume material. Crater shapes can, thus, record past epochs of high heat flows and constrain the minimum and maximum heat flows that have occurred over the surface history. The magnitude of the heat flow and the time period over which it must be applied in order to stimulate relaxation depend on several factors; all other things being equal, more relaxation will be produced in higher gravity bodies and will affect large craters more rapidly than small ones (e.g., Dombard & McKinnon 2006, Bland et al. 2012, White et al. 2017).

On several Saturnian satellites, craters exhibit variations in the ratios of their depths to their diameters, a common metric for determining the extent of relaxation. At Enceladus, Tethys, Dione, and Rhea, models of crater relaxation have provided estimates of the surface heat flows required to match the measured variations in crater shapes across each moon. Reproducing crater relaxation on Enceladus requires an extended period (~10 Myr) of high heat flow (>100 mW/m^2) and an insulating regolith that can keep the near-surface at a higher temperature than the measured surface temperature (Bland et al. 2012). Craters on Dione and Tethys record variable heat fluxes, from heavily relaxed craters that require >60 mW/m^2 to minimally relaxed craters that indicate only a few mW/m^2 (White et al. 2017). One crater on Tethys indicates an astonishing 100 mW/m^2. In contrast, Rhea's craters indicate tens of mW/m^2 with less variation in the inferred heat flux (White et al. 2013). Mimas' craters show the least relaxation among the mid-sized moons (Schenk 1989, Schenk et al. 2018), although studies have been limited. The Cassini data set enables the generation of digital elevation models from which a larger study of the depth-to-diameter ratios of Mimas' craters could be performed. Until such an analysis is complete, we must rely on models of crater modification using idealized crater shapes.

A small numerical study by Kay et al. (2022), using hypothetical crater shapes, suggests that the low gravity at Mimas would result in limited crater relaxation over timescales of a few million years. Even in the models that produced the most change in the depths of the craters, such changes would be too small to detect given the resolution of the available image data. Hence, it is plausible that the heat flow through a 24- to 29-km ice shell over an ocean would not cause detectable crater relaxation on Mimas. On the other hand, thinner ice shells produce much higher heat flows. For example, a 12-km ice shell at Mimas would produce 60 mW/m^2 (Walker & Rhoden 2022) (**Figure 3**), which has been shown to have large effects on the craters on Tethys, Dione, and Rhea (White et al. 2013, 2017). Even with Mimas' lower gravity, such a thin shell probably could not persist very long before noticeable relaxation would take place. A future study that could bound the combinations of maximum heat flow and timescale of heating would be valuable to place limits on the lifetime of the ocean and minimum thickness of the ice shell. In the meantime, the presence of an ocean and the lack of crater relaxation appear to be compatible with one another.

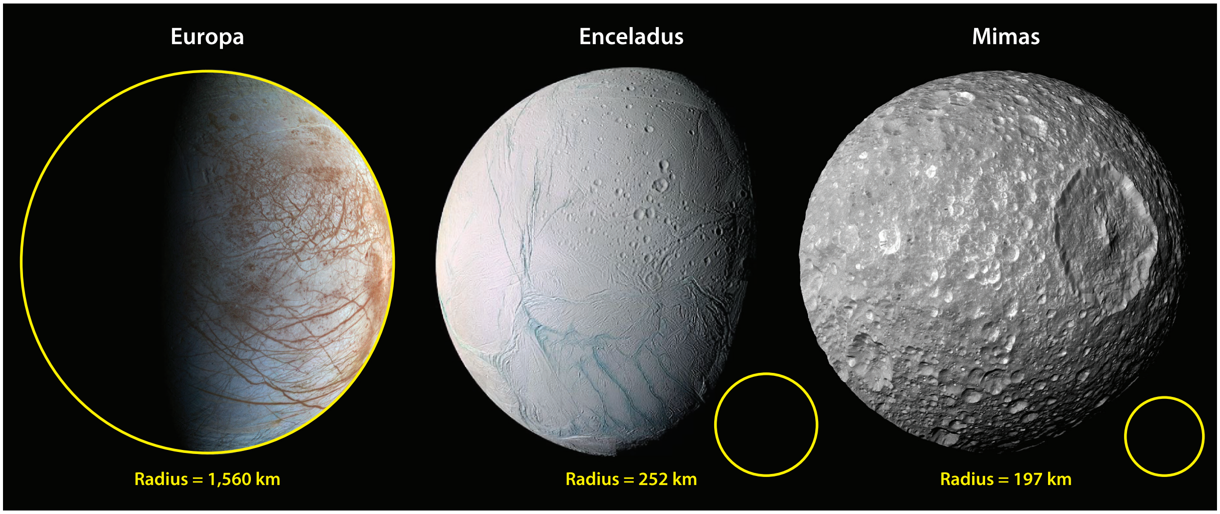

Figure 4

Confirmed ocean moons Europa (*left*) and Enceladus (*center*) display widespread tectonic activity that has been linked to tidal stress, enabled by the presence of their oceans and eccentric orbits. Mimas (*right*) has a higher eccentricity and closer orbit than either Europa or Enceladus, but its surface is heavily cratered with no indication of an ocean lurking under its ice shell. If Mimas possesses a subsurface ocean, it implies that tidal stress, alone, is insufficient to generate widespread tectonism. Here, the moons are shown at the same size to improve visibility of the geologic features. The yellow circles show the sizes of the moons, to scale.

3.1.3. Tidal stresses and Mimas' limited tectonic activity. In addition to tidal heating, an ocean-bearing Mimas will experience enhanced tidal stresses due to the response of the ocean as compared to a frozen Mimas (Rhoden et al. 2017). On confirmed ocean moons, Europa and Enceladus, tidal stresses control the orientations and distributions of tectonic features, which are widely distributed across their surfaces (**Figure 4**). In particular, the paths of arcuate fractures called cycloids, which appear to be unique to Europa, have been well matched by tracking the daily variations in tidal stress orientations and magnitudes across the surface (Greenberg et al. 1998, Hoppa et al. 2001, Rhoden et al. 2010). At Enceladus, the orientations of four long, parallel fractures at the south pole, called the Tiger Stripes, match the predicted orientations of tensile fractures formed due to tidal stress (Rhoden et al. 2020). The eruptions of Enceladus' plumes, which emanate from the Tiger Stripe Fractures, also vary in output with the tidal cycle (Hurford, et al. 2007, Nimmo et al. 2007, Hedman et al. 2013). In contrast, Mimas' surface is heavily cratered (**Figure 4**), tectonic features are sparse, and there is no evidence of eruptions, past or present (Schenk et al. 2018, and references therein). If, like Europa and Enceladus, Mimas is an ocean-bearing world in an eccentric orbit, we must ask why it lacks comparable tectonism to other ocean moons.

Rhoden et al. (2017) calculated tidal stresses in an ocean-bearing Mimas, based on the values for ice shell thickness from Tajeddine et al. (2014), using a five-layer interior model originally developed for Europa (Jara-Orué & Vermeersen 2011). They found that tidal stresses on Mimas would meet, or far exceed, those on Europa or Enceladus. Thicker, lower-viscosity ice shells could produce tidal stresses in excess of 1 MPa. Due to the limitations of the modeling approach, the study included several simplifications, including an approximation of the effects of libration, which led to an underestimate of tidal stress magnitudes. In addition, the ice shell was represented by only two layers (Rhoden et al. 2017): a brittle, high-viscosity upper layer and a ductile, low-viscosity lower layer, which is more consistent with a convecting ice shell than the conductive profile expected at Mimas (e.g., Matson et al. 2009). Because lower-viscosity ice is much more susceptible to tidal deformation at Mimas' orbital frequency, assuming a thick, low-viscosity layer will have a large effect on the tidal output (Rhoden & Walker 2022). The two-layer approximation has been shown to be sufficient for bodies with ice shells that are thin relative to the total radius of the body [e.g., at Europa (Walker & Rhoden 2022)], but such is not the case at Mimas, where even the thinnest ice shell indicated by the librations is more than 10% of its radius. Hence, tidal stress magnitudes on Mimas would likely be on the lower end of the range computed by Rhoden et al. (2017), consistent with the values found for Europa and Enceladus. Thus, the best way to reconcile an ocean within Mimas with its lack of tectonic activity would be that another source of stress has contributed to failure on Europa and Enceladus but is not available at Mimas.

While the orientations and distributions of fractures on Europa and Enceladus are clearly influenced by tidal stress, the magnitude of tidal stress, which peaks between 50 and 100 kPa depending on model parameters (e.g., Rhoden et al. 2010), is at least an order of magnitude lower than the tensile strength of pure ice in laboratory experiments (1–3 MPa) (Schulson 2006, Collins et al. 2009). It has also been suggested that stresses caused by cooling and thickening of the ice shell may play a key role in driving geologic activity (Nimmo 2004, Manga & Wang 2007, Rudolph & Manga 2009, Rudolph et al. 2022). An appealing attribute of cooling stresses is that they are isotropic in orientation. That means the orientations of fractures can be controlled by the (smaller) tidal stresses acting in concert with the (larger) cooling stresses that enable failure.

Enceladus has provided an excellent example of how cooling stresses can initiate a fracture system. Rudolph et al. (2022) tracked stress generation and fracture evolution in an Enceladus-like ice shell assuming either long-term cooling and thickening of the ice shell or an ice shell that goes through periodic cycles of warming/thinning and cooling/thickening. In both cases, during ice shell cooling, the upper portion of the ice shell undergoes increasing tensile stress associated with the volume change as ocean water gets converted to ice and from thermal stresses. Assuming a tensile failure strength of 1 or 3 MPa, failure is first achieved below the surface (~1 km depth), and the fracture then propagates radially through the ice shell in both directions. Fractures can easily reach the surface; reaching the ocean is more challenging but still possible at Enceladus due to its low gravity. Once the surface and ocean are connected by a fracture, a conduit is created by which plume eruptions can initiate.

The missing link in our understanding of the fracture system at Enceladus' south pole is how the initial radial fracture develops into a laterally propagating Tiger Stripe fracture with an orientation aligned with tidal stress (Rhoden et al. 2020). Similarly, at Europa, cooling and thickening of the ice shell can generate deep radial fractures that often reach the surface (Rudolph et al. 2022), but how these fractures enable the tidally controlled propagation of ubiquitous linear fractures or arcuate cycloids is still unclear. However the process works, the implications are the same: For Mimas to have an ocean today, tidal stresses alone cannot be responsible for fractures on icy moons. Furthermore, Mimas' ice shell could not have been cooling over its surface age. Rather, Mimas' ice shell must be warming, stable, or so early in the process of cooling that the resulting fractures have not had time to form.

To summarize, provided that Mimas' ice shell was not substantially thinner in the past, tidal heating and tidal stress are consistent with a relatively thick ice shell over a present-day ocean and satisfy the constraints that limited crater relaxation or tectonic activity are produced as a result. It is important to note, however, that a frozen Mimas with an elongated interior can also satisfy the libration measurements [although perhaps not as well as the ocean model (see Noyelles 2017, Caudal 2017)], and the resulting lack of tidal responsiveness could account for the limited crater relaxation and lack of tectonic activity.

3.2. The Herschel-Forming Impact and the Evolution of a Mimean Ocean

The Herschel impact basin is the most iconic feature on Mimas. Its diameter spans ~140 km, and it has an estimated depth of ~10 km (Schenk et al. 2018). The age of Herschel is uncertain, but crater counts within the basin suggest its interior is one of the youngest regions of Mimas (Kirchoff et al. 2018). The basin displays a typical morphology, with a well-defined central peak. Herschel's morphology gives no indication of a subsurface ocean (cf. Turtle & Pierazzo 2001, Silber & Johnson 2017), which suggests that the ice shell was thick enough at the time of impact that the ocean had little effect on the formation of the basin.

Due to the complexities of modeling large basins, particularly into ice, studies of the Herschel-forming impact have historically been limited. Only recently have the tools needed to properly treat large impacts into small, icy moons become available. Bruesch & Asphaug (2014) used a smooth particle hydrodynamics model to simulate a Herschel-like impact into a body with Mimas-like dimensions to determine whether disrupted terrains ought to be expected on the antipode of Herschel. They modeled only one impactor size and velocity ($D = 2.9$ km, $v_{imp} = 20$ km/s), and they did not analyze the morphology of the resulting basin. Rather, they focused on how seismic energy from the impact would be affected by different properties of Mimas' core.

Denton & Rhoden (2022) modeled the formation of Herschel in an ice shell over an ocean using the finite element software iSALE (Amsden et al. 1980, Collins et al. 2004, Wünnemann et al. 2006). They adopted standard material parameters and equations of state to describe the behavior of the ice and ocean, and assumed an icy impactor with an impact velocity of 15 km/s, which is appropriate for a planetocentric impactor. Although the provenance of the Herschel-forming impactor is unknown, there is substantial evidence that planetocentric debris has heavily contributed to cratering on Saturn's mid-sized moons (e.g., Kirchoff et al. 2018; Ferguson et al. 2020, 2022a,b). Furthermore, Mimas' small size, along with the large gravitational focusing of Saturn at Mimas' orbital distance, leads to highly energetic heliocentric impacts that would be likely to obliterate Mimas (e.g., Movshovitz et al. 2015). Using existing scaling laws and preliminary simulations, Denton & Rhoden (2022) determined that the impactor size at this velocity would need to be ~4.8 km.

All simulations adopted a surface temperature of 80 K and a temperature at the base of the ice shell of 273 K, but several thermal profiles were tested, including fully conductive, conductive for up to 50 km with an isothermal layer below that depth, and a conductive profile for 90% of the ice shell and isothermal profile for the bottom 10%. Although Mimas is likely too small for its ice shell to convect (Matson et al. 2009), tidal heating will result in an isothermal layer at the shell base because heating is concentrated in the lower-viscosity ice located there, thus mimicking the behavior of a thin convecting layer (Walker & Rhoden 2022).

Using 2D simulations of an impact into a flat surface as an initial point of study, Denton & Rhoden (2022) began with a 30-km-thick ice shell over an ocean 40 km deep, which is consistent with the libration measurements (Tajeddine et al. 2014) and just above the range indicated by the tidal heating analysis (Rhoden & Walker 2022). They then increased the ice shell thickness up to 70 km (essentially, a fully frozen Mimas) to identify changes in the resulting crater morphology. At 30 km, the ice shell is obliterated at the impact site, and the resulting morphology of the basin is inconsistent with that of Herschel (**Figure 5**, *left*). However, if the ice shell is increased to 55-km thickness (**Figure 5**, *center*), the shape of the resulting basin is indistinguishable from an impact into a frozen Mimas (**Figure 5**, *right*). These results strongly suggest that, at the time of the Herschel-forming impact, Mimas' ice shell was at least 55 km thick, which is about double the present-day estimate. The resulting implication is that, for Mimas to have an ocean today, the ice shell has been thinning since the formation of Herschel from ~55 km to less than 30 km.

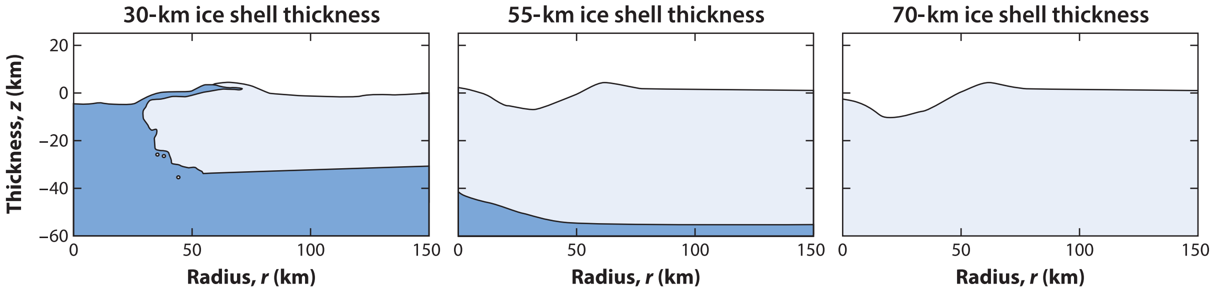

Figure 5

Simulations of the Herschel-forming impact using iSALE, assuming an ice shell (*light blue*) over an ocean (*dark blue*) with varying shell thicknesses. The results show that a 30-km-thick ice shell would not have survived the impact (*left*). Only when the ice shell is at least 55 km thick can the morphology of Herschel be reproduced (*center*); thicker shells do not result in major changes to the crater morphology. Therefore, if Mimas has an ocean today, the ice shell had to have been tens of kilometers thicker when Herschel formed. Interestingly, only simulations that included an isothermal layer at the base of the ice shell were able to create a central uplift, consistent with observations of Herschel. An isothermal layer is a natural outcome of tidal dissipation in the ice shell, which is concentrated in the warm ice near the shell base (Rhoden & Walker 2022), suggesting that the ocean had to exist when the Herschel-forming impact occurred. However, it is possible that some simplification in the numerical modeling approach is restricting formation of a central uplift in fully conductive shells, so additional work is needed to confirm this result. Figure adapted from Denton & Rhoden (2022).

Another interesting finding by Denton & Rhoden (2022) was that the fully conductive thermal profiles failed to reproduce the interior morphology of Herschel, likely because the ice is too hard. When an underlying isothermal layer is included, the central uplift within the basin is reproduced, as long as the ice shell is thick enough to withstand the impact. Given the low likelihood of convection at Mimas, and the fact that tidal heating is the only readily available heat source at present, the isothermal layer is best explained as the result of tidal heating. An important implication of this finding is that Mimas was not frozen when Herschel formed. Rather, the ocean had to exist in order to generate tidal heating that warmed the lower portion of the ice shell. Although the impact modeling study was limited in scope, this provocative result motivates a more in-depth future study and makes the ocean hypothesis even more plausible.

3.3. Saturn's Rings and the Recent Orbital Evolution of Mimas and Enceladus

3.3.1. A new view of Saturn's quality factor, *Q*. For a moon orbiting close enough to be influenced by tides, thermal evolution can be strongly affected by orbital evolution, particularly by mean motion resonances (commensurabilities in orbital period) with other moons in the system (e.g., Peale et al. 1979, Schubert et al. 2010). Even temporary capture into a resonance can substantially alter the eccentricity of a moon, stimulating a larger tidal response. By integrating the orbits of moons backward through time, it is possible to trace the history of resonance passages, placing constraints on the eccentricities and extent of past tidal heating within the moons (e.g., Ćuk et al. 2016). However, our ability to rewind the thermal-orbital history of Saturn's mid-sized moons has been complicated by new discoveries regarding tidal dissipation within Saturn, which is represented by the quality factor (Q).

Saturn's Q controls the timescale of orbital evolution of its moons, which in turn affects the history of mean motion resonances and the eccentricity evolution of the moons. In the past, Q was assumed to be large (of order 10,000) and constant (e.g., Meyer & Wisdom 2008). Using the old value, the mid-sized moons would have to have formed billions of years ago in order to have time to migrate outward to their current locations (e.g., Neveu & Rhoden 2019). Assuming a constant Q meant the locations of potential mean motion resonances were straightforward to predict, providing constraints on the dynamical histories of the moons. When applied to the mid-sized moons of Saturn, Ćuk et al. (2016) identified a resonance passage that would have trapped the moons in a resonance that they do not currently occupy. The only reasonable explanation seemed to be that the moons were extremely young, less than 100 Myr old, such that they had yet to encounter the troublesome resonance. However, a new discovery provided a different explanation for how the moons avoided the resonance, lifting the constraint of an extremely young age for the moons.

Using a combination of a century's worth of astrometry measurements and Cassini data, Lainey et al. (2017, 2020) showed that Saturn's Q is actually low and frequency dependent, which means that, as a moon's orbital distance changes, the tidal response of Saturn that it experiences can also change. As a consequence, the rate of expansion of a moon's orbit can increase and decrease with time, and each of Saturn's moons can be subject to a different effective Q of Saturn. We now understand that Saturn's Q is linked to the atmospheric layers and dynamics within Saturn, a mechanism described as resonance locking (e.g., Fuller et al. 2016; Nimmo et al. 2018, and references therein; Lainey et al. 2020), so dissipation may even change over time. Our new understanding of Q complicates dynamical models of the moons' coevolution, making it much more difficult to know what resonance passages occurred, and the resulting orbital changes that would have resulted. Hence, we must rely on other observational constraints on the orbital evolutions of the mid-sized moons.

3.3.2. Forming the Cassini Division. Within Saturn's rings, centered at ~2 R_S, there is an ~4,600-km gap known as the Cassini Division (**Figure 6**). The origin of the gap was initially explained within the old paradigm of constant, low dissipation within Saturn and a primordial system of rings and moons (e.g., Goldreich & Tremaine 1978). With our new understanding of Saturn's Q (Fuller et al. 2016, Lainey et al. 2017, Nimmo et al. 2018), the formation of the Cassini Division has been revisited. Baillié et al. (2019) determined that inward migration of Mimas could drive open a gap in the rings, consistent with the width of the Cassini Division. Although moons

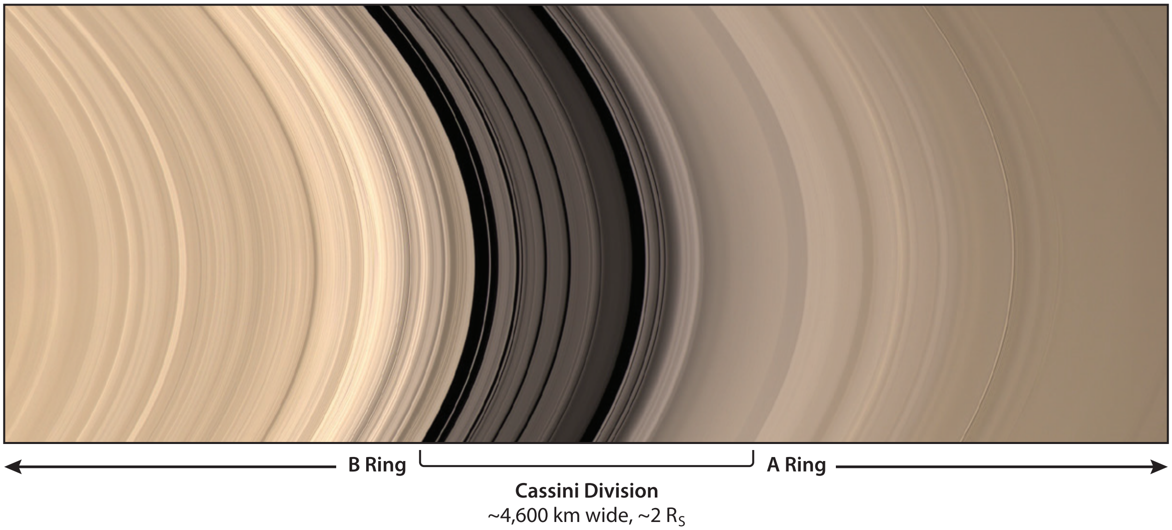

Figure 6

The Cassini Division is a large gap between the A and B rings, as shown in this annotated Cassini image of Saturn's rings. Inward migration of Mimas (presently orbiting at ~3 R_S, so not visible here), due to a temporary resonance with Enceladus, could have opened the gap relatively recently in Solar System history, providing a potential pathway to enhance tidal heating and generate oceans within Mimas and Enceladus. Photo PIA11142, courtesy of NASA/JPL/Space Science Institute.

typically migrate outward from their host planet over time, the variable migration rates caused by the frequency dependence of Saturn's Q could have led Mimas to enter a temporary mean motion resonance with Enceladus that caused it to migrate inward and dramatically increased its eccentricity. It is assumed that, eventually, tidal heating from the high-eccentricity, close orbit became high enough to trigger melting within Mimas, changing the way dissipation was partitioned between the moons and the orbits, and ultimately breaking the resonance. Mimas then resumed its initial outward migration, with its eccentricity rapidly decreasing to the present-day value.

Models of the thermal evolution of Mimas and Enceladus during the formation of the Cassini Division have explored only two end-member cases (Noyelles et al. 2019), in which all of the tidal dissipation occurs in only one of the moons and the entire process takes place within the past ~10 million years. Neither case simultaneously reproduces the current orbital elements and the inferred interior structures of the moons. In particular, to reproduce the Cassini Division, Mimas would have fully melted within the past ~10 Myr (Noyelles et al. 2019), which conflicts with its heavily cratered surface. However, the 10 Myr timescale is based on model assumptions regarding the proportion of the gap that is caused by the interactions with Mimas and the timescales over which the Cassini Division is created and filled in. These parameters are sensitive to the assumed age of the rings, the rate of viscous spreading of the rings, the rate at which material is added to the rings, etc. Thus, it seems plausible that the mechanism described by Baillié et al. (2019) and Noyelles et al. (2019) could have occurred on a somewhat longer timescale than 10 Myr.

It is important to consider whether the formation of the Cassini Division through recent inward migration of Mimas, and the corresponding thermal-orbital evolution of Mimas and Enceladus, would be compatible with the geologic histories of the moons. The first area of concern is that the model implies that Mimas' eccentricity has been decreasing since the onset of melting in the interior. A decreasing eccentricity ought to reduce tidal heating over Mimas' recent past, cooling the interior and leading to thickening of the ice shell, thinning of the ocean, and large stresses. Mimas' geology appears to tell the opposite story, in which the ice shell has been thinning, at least since the formation of Herschel, which could have easily occurred more than 10 Myr ago.

The solution may be the time it takes for the ice shell to respond to changes in tidal dissipation. If Mimas began frozen, and the increase in eccentricity triggered melting that formed a nascent ocean, the ice shell would immediately be out of thermal equilibrium. The eccentricity at the onset of melting could conceivably produce enough heat to entirely melt the ice shell, but the shell would be starting at a thickness of nearly 70 km. There would, thus, be a competition between the ice shell moving toward the equilibrium thickness by melting/thinning and the equilibrium thickness increasing as the eccentricity drops. The timescale for the ice shell to evolve from a state of melting to one of thermal equilibrium is not yet known. The timescale is coupled to the eccentricity evolution, making it a complex numerical problem to model. The tidal heating analysis by Rhoden & Walker (2022) along with the libration models allow for a thick (<30 km) ice shell in thermal equilibrium today. Future work to model the competing processes of decreasing eccentricity and ice shell melting would provide an upper limit on the time period over which Mimas' migration occurred. In turn, that limit can be used as a constraint on the age of the Cassini Division. Rather than beginning with the assumption of a 10 Myr age for the onset of inward migration, these models could provide a different, geologically informed initial condition to test.

The inward migration model for forming the Cassini Division also has geologic implications for Enceladus. Similar to Mimas, Enceladus would undergo a late epoch of high eccentricity that could initiate melting and ocean formation. There is some independent evidence to support such a scenario. While the south polar fracture system is the most extensive, and perhaps only active, geologic region on Enceladus, there are also tectonized regions near the leading and trailing points, along Enceladus' equator (Crow-Willard & Pappalardo 2015). The fractures at the equator are older than the south polar features, and there are no eruptions at present or clear evidence of past eruptions. Rhoden et al. (2020) attempted to explain the formation of all three tectonized regions within the context of Enceladus' overall evolution. They pointed out that the global pattern of tidal stress in a frozen Enceladus would concentrate stress at the locations of the equatorial tectonized regions, whereas, in an ocean-bearing Enceladus, the tidal stresses are highest at the poles (see also Roberts 2015). They suggested that Enceladus underwent an episode of melting, transitioning from a frozen hydrosphere in contact with the rocky interior to a global ocean moon, thereby changing the locations at which tidal tectonics would be active.

Within this framework, Enceladus would eventually have to cool down in order to generate the cooling stresses invoked to explain the formation of the plume conduits associated with the Tiger Stripe Fractures (as in Rudolph et al. 2022). Furthermore, the entire evolution of the ice shell would have had to have occurred recently enough for the older tectonized terrains to still be preserved in the geologic record. Particles erupted from the plumes of Enceladus include the products of hydrothermal alteration (Postberg et al. 2018, and references therein), which occurs rapidly when liquid water is in contact with dry rock, supporting the idea that the ocean is relatively young. Formation of the Cassini Division provides a mechanism to first increase tidal heating and stimulate ocean development and then reduce tidal heating, leading to cooling and thickening of the ice shell, within the geologically recent past.

4. CONSTRUCTING A SELF-CONSISTENT HISTORY OF AN OCEAN-BEARING MIMAS

Given all of the geologic and dynamic information described in the preceding sections, a pathway to late emergence of an ocean-bearing Mimas is becoming clear. At some point in Mimas' history, it was layered but frozen. It encountered a resonance with Enceladus that caused it to migrate toward Saturn, opening the Cassini Division, and increasing Mimas' eccentricity substantially. The high eccentricity triggered melting at the rock-ice interface, which eventually formed a thin global ocean. As a result, tidal heating was greatly enhanced, and the ice shell began producing far more tidal heat than it could transport out. Since the formation of the ocean, Mimas' ice shell has been melting, even as its eccentricity has been decreasing. The Herschel-forming impact occurred sometime after the ocean formed but early enough that the ice shell was still ~55 km or thicker. At some point in the recent past, Mimas' ice shell evolved to a point of stable thermal equilibrium at a thickness of 24–29 km. Because the ice shell has been thinning, rather than thickening, cooling stresses have not been available to generate sufficient tensile stress to drive observable fracture formation on Mimas. Also, the heat flow available to relax craters is low, and the ocean may be young relative to the surface age, such that there may have been insufficient time to cause detectable relaxation.

It is possible that a similar evolution took place at Enceladus, where the increase in eccentricity during inward migration increased tidal heating sufficiently to melt the ice shell and form an ocean. Because Enceladus has a substantially larger core than Mimas, heat from dissipation within the core, as well as from the exothermal hydration reactions at the rock-ocean interface, could explain the substantially higher heat flows recorded at Enceladus versus Mimas. If Enceladus was able to reach its equilibrium ice shell thickness sooner than Mimas, and further reductions in eccentricity have put it into a state of ice shell thickening, it could explain why Enceladus has developed the south polar fracture system and active plumes while Mimas has stayed quiescent. While speculative, this hypothesis implies that Mimas and Enceladus represent two stages along the same evolutionary path, suggesting that, in the future, Mimas may display the same type of activity that Enceladus exhibits today.

It is also useful to consider the implications of this proposed recent history of Mimas on its formation and ancient history. After the formation of Saturn and its CPD, ~4 Gyr ago, Mimas either formed layered from the rings (as in Charnoz et al. 2011) or was heated sufficiently to induce global differentiation after formation by standard accretion in the CPD (e.g., Neveu & Rhoden 2017). In either case, Mimas likely ended up in a low-eccentricity orbit, with an ice shell over a relatively rocky interior. In a standard accretion model, melting-induced differentiation would have occurred, and ceased, very early (Neveu & Rhoden 2017). Given the ongoing hydrothermal alteration activity at Enceladus (Postberg et al. 2018), and the apparent need for a porous, mixed ice-rock interior for Enceladus to produce extensive tidal heating (Roberts 2015, Choblet et al. 2017, Liao et al. 2020, Rovira-Navarro et al. 2022), the ring formation model is favored over standard accretion.

Both formation models imply that Mimas had a layered interior at some point after its initial assembly. However, between the assembly of Mimas and the initiation of the Cassini Division migration, Mimas would have been subjected to bombardment that cratered its surface. If Mimas initially assembled in the CPD, the bombardment period would have lasted billions of years, making it likely that a precursor body was disrupted and reassembled to form the present-day Mimas (as in Ćuk et al. 2016), although an initially differentiated structure may limit the extent of disruptive impacts (e.g., Movshovitz et al. 2015). In contrast, within the ring formation model, Mimas would be the youngest of the mid-sized moons, perhaps providing a pathway by which it can avoid disruptive impacts. An interesting potential avenue of future work would be to determine whether an initial layered structure would result in a different interior evolution through the Cassini Division migration than a more homogenous interior. If the initial interior has a strong effect on the overall heat budget, final structure, or geology, it could provide a way to determine whether Mimas was ever disrupted, with implications for its lifetime and mechanism of formation.

5. CONCLUSIONS AND FUTURE DIRECTIONS

Although a subsurface ocean beneath a thick ice shell can explain Mimas' librations (Tajeddine et al. 2014), the ocean interpretation was received with skepticism due to the lack of surface features on Mimas that are observed on other icy, ocean worlds, despite Mimas' high potential for tidal activity (e.g., Rhoden et al. 2017) (**Figure 4**). However, as described in the preceding sections, Mimas' geology is consistent with a young ocean and an ice shell that has been thinning since at least the formation of Herschel. Although a frozen Mimas cannot be completely ruled out by the geology (the Herschel models notwithstanding), no geologic features have yet been identified that can rule out a young ocean.

The new paradigm of a frequency-dependent Q of Saturn (Fuller et al. 2016; Lainey et al. 2017, 2020; Nimmo et al. 2018) has vastly widened the suite of possible formation mechanisms for the mid-sized moons and their later evolutionary pathways. The moons may be significantly younger than Saturn, perhaps even spawned from Saturn's rings (Charnoz et al. 2011, Salmon & Canup 2017). The thermal evolution of moons formed in this manner has not been fully explored. In particular, whether the composition and properties of the cores of ring-born moons would produce the enhanced tidal heating observed at Enceladus has yet to be determined. Much less is known about the core of Mimas. If it is similar to the fluffy core of Enceladus (Roberts 2015), there may be much greater potential to generate tidal heat and initiate melting than has been assumed in past thermal-orbital evolution models.

A recent model for the formation of the Cassini Division (Baillié et al. 2019, Noyelles et al. 2019) requires a resonance between Mimas and Enceladus that would have caused a fundamental change in their tidal heating budgets in the recent past. Connecting these conditions with the geology and interiors of both moons provides a plausible pathway for achieving a late-stage ocean within Mimas. Furthermore, differences in the levels of geologic activity between Mimas and Enceladus may also be explained if Enceladus' ice shell is thickening as it moves toward a new thermal equilibrium while Mimas' ice shell is at or near a state of thermal equilibrium with its present-day eccentricity.

If the ocean hypothesis could be confirmed by other measurements or observations, it would provide motivation to further explore mechanisms for late-stage ocean formation within mid-sized moons. If Mimas were shown to be frozen today, a ring formation model is preferred over formation in the CPD, as it avoids warming, tidal runaway, and circularization while producing the required layering to match the libration measurements. The role of disruptive impacts and reassembly is critical to explore in either case, as well as the coupled evolution of the orbits and ice shells of Mimas and Enceladus through the creation of the Cassini Division.

While ocean detection from remote sensing is challenging, and often requires multiple types of data collection, the relationship between ice shell thickness and surface heat flow, identified by Rhoden & Walker (2022), offers a method for differentiating between a frozen and an ocean-bearing Mimas through a measurement of surface heat flow. For the parameters in their study, an ocean-bearing Mimas with an ice shell <30 km thick should have a heat flow of at least four times that of a frozen Mimas, which may be detectable by spacecraft instrumentation. Although Mimas' surface makes it appear much less enticing than its neighbor, Enceladus, our new perspective on Mimas suggests it is one of the youngest ocean moons in the outer Solar System, with a fascinating history (and perhaps even more fascinating future) that must be explored.

DISCLOSURE STATEMENT

The author is not aware of any affiliations, memberships, funding, or financial holdings that might be perceived as affecting the objectivity of this review.

ACKNOWLEDGMENTS

The author wishes to thank Julien Salmon and Sierra Ferguson for assistance in developing this review and the attendees of the International Space Science Institute Workshop "New vision of the Saturnian system in the context of a highly dissipative Saturn" for stimulating discussions related to the formation and evolution of Saturn's mid-sized moons. This work was supported through NASA grants related to the evolution of icy, ocean moons (80NSSC19K0557 and NNX17AG01G) and the efforts of Stan Sajous and Morghan Rogers, who enable me to be a good mom while also being a scientist.

LITERATURE CITED

Amsden AA, Ruppel HM, Hirt CW. 1980. *SALE: a simplified ALE computer program for fluid flow speeds*. Tech. Rep. 5176006, Los Alamos Sci. Lab., Los Alamos, NM. **https://doi.org/https://doi.org/10.2172/5176006**

Asphaug E, Reufer A. 2013. Late origin of the Saturn system. *Icarus* 223:544–65

Baillié K, Noyelles B, Lainey V, Charnoz S, Tobie G. 2019. Formation of the Cassini Division—I. Shaping the rings by Mimas inward migration. *Mon. Not. R. Astron. Soc.* 486:2933–46

Bland MT, Singer KN, McKinnon WB, Schenk PM. 2012. Enceladus' extreme heat flux as revealed by its relaxed craters. *Geophys. Res. Lett.* 39:L17204

Bottke WF, Brož M, O'Brien DP, Bagatin AC, Morbidelli A, Marchi S. 2015. The collisional evolution of the main asteroid belt. In *Asteroids IV*, ed. P Michel, FE Demeo, WF Bottke, pp. 701–24. Tucson: Univ. Arizona Press

Bruesch LS, Asphaug E. 2004. Modeling global impact effects on middle-sized icy bodies: applications to Saturn's moons. *Icarus* 168:457–66

Canup RM, Ward WR. 2006. A common mass scaling for satellite systems of gaseous planets. *Nature* 441:834–39

Castillo-Rogez JC, Efroimsky M, Lainey V. 2011. The tidal history of Iapetus: spin dynamics in the light of a refined dissipation model. *J. Geophys. Res.* 116(E9):E09008

Castillo-Rogez JC, Hemmingway D, Rhoden AR, Tobie G, McKinnon WB. 2018. Origin and evolution of Saturn's mid-sized moons. In *Enceladus and the Icy Moons of Saturn*, ed. PM Schenk, RN Clark, CJA Howett, AJ Verbiscer, JH Waite, pp. 285–306. Tucson: Univ. Arizona Press

Caudal G. 2017. The damping of forced librations of triaxial satellites with eccentric orbits: consequences on the dynamics of Mimas. *Icarus* 286:280–88

Charnoz S, Crida A, Castillo-Rogez JC, Lainey V, Dones L, et al. 2011. Accretion of Saturn's mid-sized moons during the viscous spreading of young massive rings: solving the paradox of silicate-poor rings versus silicate-rich moons. *Icarus* 216:535–50

Choblet G, Tobie G, Sotin C, Běhounková M, Čadek O, et al. 2017. Powering prolonged hydrothermal activity inside Enceladus. *Nat. Astron.* 1:841–47

Collins GC, McKinnon WB, Moore JM, Nimmo F, Pappalardo RT, et al. 2009. Tectonics of the outer planet satellites. In *Planetary Tectonics*, ed. TR Watters, RA Schultz, pp. 264–350. Cambridge, UK: Cambridge Univ. Press

Collins GS, Melosh HJ, Ivanov BA. 2004. Modeling damage and deformation in impact simulations. *Meteorit. Planet. Sci.* 39:217–31

Colwell JE, Nicholson PD, Tiscareno MS, Murray CD, French RG, Marouf EA. 2009. The structure of Saturn's rings. In *Saturn from Cassini-Huygens*, ed. MK Dougherty, LW Esposito, SM Krimigis, pp. 375–412. Dordrecht, Neth.: Springer

Crow-Willard EN, Pappalardo RT. 2015. Structural mapping of Enceladus and implications for formation of tectonized regions. *J. Geophys. Res. Planets* 120:928–50

Ćuk M, Dones L, Nesvorný D. 2016. Dynamical evidence for a late formation of Saturn's moons. *Astrophys. J.* 820:97

Denton CA, Rhoden AR. 2022. Tracking the evolution of an ocean within Mimas using the Herschel impact basin. *Geophys. Res. Lett.* 49(24):e2022GL100516

Dombard AJ, McKinnon WB. 2006. Elastoviscoplastic relaxation of impact crater topography with application to Ganymede and Callisto. *J. Geophys. Res.* 111(E1):E01001

Dubinski J. 2019. A recent origin for Saturn's rings from the collisional disruption of an icy moon. *Icarus* 321:291–306

Ferguson SN, Rhoden AR, Kirchoff MR. 2020. Small impact crater populations on Saturn's moon Tethys and implications for source impactors in the system. *J. Geophys. Res. Planets* 125:e2020JE006400

Ferguson SN, Rhoden AR, Kirchoff MR. 2022a. Regional impact crater mapping and analysis on Saturn's moon Dione and the relation to source impactors. *J. Geophys. Res. Planets* 127:e2022JE007204

Ferguson SN, Rhoden AR, Kirchoff MR, Salmon JJ. 2022b. A unique Saturnian impactor population from elliptical craters. *Earth Planet. Sci. Lett.* 593:117652

Fuller J, Luan J, Quataert E. 2016. Resonance locking as the source of rapid tidal migration in the Jupiter and Saturn moon systems. *Mon. Not. R. Astron. Soc.* 458:3867–79

Goldreich P, Tremaine S. 1978. The formation of the Cassini division in Saturn's rings. *Icarus* 34:240–53

Greenberg R, Geissler P, Hoppa G, Tufts BR, Durda DD, et al. 1998. Tectonic processes on Europa: tidal stresses, mechanical response, and visible features. *Icarus* 135:64–78

Greenstreet S, Gladman B, McKinnon WB. 2015. Impact and cratering rates onto Pluto. *Icarus* 258:267–88

Hedman MM, Gosmeyer CM, Nicholson PD, Sotin C, Brown RH, et al. 2013. An observed correlation between plume activity and tidal stresses on Enceladus. *Nature* 500:182–84

Hiesinger H, van der Bogert CH, Pasckert JH, Funcke L, Giacomini L, et al. 2012. How old are young lunar craters? *J. Geophys. Res.* 117(E12):E00H10

Hoppa GV, Greenberg R, Riley J, Tufts BR. 2001. Observational selection effects in Europa image data: identification of chaotic terrain. *Icarus* 151:181–89

Howett CJA, Spencer JR, Schenk P, Johnson RE, Paranicas C, et al. 2011. A high-amplitude thermal inertia anomaly of probable magnetospheric origin on Saturn's moon Mimas. *Icarus* 216:221–26

Hurford TA, Helfenstein P, Hoppa GV, Greenberg R, Bills BG. 2007. Eruptions arising from tidally controlled periodic openings of rifts on Enceladus. *Nature* 447:292–94

Hussmann H, Sotin C, Lunine JI. 2015. Interiors and evolution of icy satellites. *Treatise Geophys.* 10:605–35

Jara-Orué HM, Vermeersen BLA. 2011. Effects of low-viscous layers and a non-zero obliquity on surface stresses induced by diurnal tides and non-synchronous rotation: the case of Europa. *Icarus* 215:417–38

Kay JP, Rhoden AR, Walker ME. 2022. *Using the lack of relaxation on Mimas to test for an ocean*. Paper presented at the 53rd Lunar and Planetary Science Conference, Woodlands, TX, March 7–11

Kirchoff MR, Bierhaus EB, Dones L, Singer KN, Robbins SJ, et al. 2018. Cratering histories in the Saturnian system. In *Enceladus and the Icy Moons of Saturn*, ed. PM Schenk, RN Clark, CJA Howett, AJ Verbiscer, JH Waite, pp. 267–84. Tucson: Univ. Arizona Press

Lainey V, Casajus LG, Fuller J, Zannoni M, Tortora P, et al. 2020. Resonance locking in giant planets indicated by the rapid orbital expansion of Titan. *Nat. Astron.* 4:1053–58

Lainey V, Jacobson RA, Tajeddine R, Cooper NJ, Murray C, et al. 2017. New constraints on Saturn's interior from Cassini astrometric data. *Icarus* 281:286–96

Liao Y, Nimmo F, Neufeld JA. 2020. Heat production and tidally driven fluid flow in the permeable core of Enceladus. *J. Geophys. Res. Planets* 125:e2019JE006209

Manga M, Wang CY. 2007. Pressurized oceans and the eruption of liquid water on Europa and Enceladus. *Geophys. Res. Lett.* 34:L07202

Matson DL, Castillo-Rogez JC, Schubert G, Sotin C, McKinnon WB. 2009. The thermal evolution and internal structure of Saturn's mid-sized icy satellites. In *Saturn from Cassini-Huygens*, ed. MK Dougherty, LW Esposito, SM Krimigis, pp. 577–612. Dordrecht, Neth.: Springer

Meyer J, Wisdom J. 2008. Tidal evolution of Mimas, Enceladus, and Dione. *Icarus* 193:213–23

Movshovitz N, Nimmo F, Korycansky DG, Asphaug E, Owen JM. 2015. Disruption and reaccretion of midsized moons during an outer solar system Late Heavy Bombardment. *Geophys. Res. Lett.* 42:256–63

NASEM (Natl. Acad. Sci. Eng. Med.). 2022. *Origins, Worlds, and Life: A Decadal Strategy for Planetary Science and Astrobiology 2023–2032*. Washington, DC: Natl. Acad.

Neukum G, Ivanov BA, Hartmann WK. 2001. Cratering records in the inner solar system in relation to the lunar reference system. *Space Sci. Rev.* 96:55–86

Neveu M, Rhoden AR. 2017. The origin and evolution of a differentiated Mimas. *Icarus* 296:183–96

Neveu M, Rhoden AR. 2019. Evolution of Saturn's mid-sized moons. *Nat. Astron.* 3:543–52

Nimmo F. 2004. Stresses generated in cooling viscoelastic ice shells: application to Europa. *J. Geophys. Res.* 109:E12001

Nimmo F, Barr AC, Behounkova M, McKinnon WB. 2018. The thermal and orbital evolution of Enceladus: observational constraints and models. *Enceladus and the Icy Moons of Saturn*, ed. PM Schenk, RN Clark, CJA Howett, AJ Verbiscer, JH Waite, pp. 79–94. Tucson: Univ. Arizona Press

Nimmo F, Korycansky DG. 2012. Impact-driven ice loss in outer Solar System satellites: consequences for the Late Heavy Bombardment. *Icarus* 219:508–10

Nimmo F, Spencer JR, Pappalardo RT, Mullen ME. 2007. Shear heating as the origin of the plumes and heat flux on Enceladus. *Nature* 447:289–91

Noyelles B. 2017. Interpreting the librations of a synchronous satellite—how their phase assesses Mimas' global ocean. *Icarus* 282:276–89

Noyelles B, Baillié K, Charnoz S, Lainey V, Tobie G. 2019. Formation of the Cassini Division—II. Possible histories of Mimas and Enceladus. *Mon. Not. R. Astron. Soc.* 486:2947–63

Peale SJ. 1999. Origin and evolution of the natural satellites. *Annu. Rev. Astron. Astrophys.* 37:533–602

Peale SJ, Cassen P, Reynolds RT. 1979. Melting of Io by tidal dissipation. *Science* 203:892–94

Porco CC, Helfenstein P, Thomas PC, Ingersoll AP, Wisdom J, et al. 2006. Cassini observes the active south pole of Enceladus. *Science* 311:1393–401

Postberg F, Clark RN, Hansen CJ, Coates AJ, Dalle Ore CM, et al. 2018. Plume and surface composition of Enceladus. In *Enceladus and the Icy Moons of Saturn*, ed. PM Schenk, RN Clark, CJA Howett, AJ Verbiscer, JH Waite, pp. 129–62. Tucson: Univ. Arizona Press

Rhoden AR, Henning W, Hurford TA, Patthoff DA, Tajeddine R. 2017. The implications of tides on the Mimas ocean hypothesis. *J. Geophys. Res. Planets* 122:400–10

Rhoden AR, Hurford TA, Spitale J, Henning W, Huff EM, et al. 2020. The formation of Enceladus' Tiger Stripe Fractures from eccentricity tides. *Earth Planet. Sci. Lett.* 544:116389

Rhoden AR, Militzer B, Huff EM, Hurford TA, Manga M, Richards MA. 2010. Constraints on Europa's rotational dynamics from modeling of tidally-driven fractures. *Icarus* 210:770–84

Rhoden AR, Walker ME. 2022. The case for an ocean-bearing Mimas from tidal heating analysis. *Icarus* 376:114872

Roberts JH. 2015. The fluffy core of Enceladus. *Icarus* 258:54–66

Rovira-Navarro M, Katz RF, Liao Y, van der Wal W, Nimmo F. 2022. The tides of Enceladus' porous core. *J. Geophys. Res. Planets* 127:e2021JE007117

Rudolph ML, Manga M. 2009. Fracture penetration in planetary ice shells. *Icarus* 199:536–41

Rudolph ML, Manga M, Walker M, Rhoden AR. 2022. Cooling crusts create concomitant cryovolcanic cracks. *Geophys. Res. Lett.* 49(5):e2021GL094421

Salmon J, Canup RM. 2017. Accretion of Saturn's inner mid-sized moons from a massive primordial ice ring. *Astrophys. J.* 836:109

Schenk P, White OL, Byrne PK, Moore JM. 2018. Saturn's other icy moons: geologically complex worlds in their own right. In *Enceladus and the Icy Moons of Saturn*, ed. PM Schenk, RN Clark, CJA Howett, AJ Verbiscer, JH Waite, pp. 237–65. Tucson: Univ. Arizona Press

Schenk PM. 1989. Crater formation and modification on the icy satellites of Uranus and Saturn: depth/diameter and central peak occurrence. *J. Geophys. Res.* 94(B4):3813–32

Schubert G, Hussmann H, Lainey V, Matson DL, McKinnon WB, et al. 2010. Evolution of icy satellites. *Space Sci. Rev.* 153:447–84

Schulson EM. 2006. The fracture of water ice Ih: a short overview. *Meteorit. Planet. Sci.* 41:1497–508

Silber EA, Johnson BC. 2017. Impact crater morphology and the structure of Europa's ice shell. *J. Geophys. Res. Planets* 122:2685–701

Singer KN, McKinnon WB, Gladman B, Greenstreet S, Bierhaus EB, et al. 2019. Impact craters on Pluto and Charon indicate a deficit of small Kuiper belt objects. *Science* 363:955–59

Spencer JR, Pearl JC, Segura M, Flasar FM, Mamoutkine A, et al. 2006. Cassini encounters Enceladus: background and the discovery of a south polar hot spot. *Science* 311:1401–5

Tajeddine R, Rambaux N, Lainey V, Charnoz S, Richard A, et al. 2014. Constraints on Mimas' interior from Cassini ISS libration measurements. *Science* 346:322–24

Turtle EP, Pierazzo E. 2001. Thickness of a Europan ice shell from impact crater simulations. *Science* 294:1326–28

Walker ME, Rhoden AR. 2022. Tidal heating at Europa using the multifrequency analysis of tidal heating toolkit. *Planet. Sci. J.* 3:149

White OL, Schenk PM, Bellagamba AW, Grimm AM, Dombard AJ, Bray VJ. 2017. Impact crater relaxation on Dione and Tethys and relation to past heat flow. *Icarus* 288:37–52

White OL, Schenk PM, Dombard AJ. 2013. Impact basin relaxation on Rhea and Iapetus and relation to past heat flow. *Icarus* 223:699–709

Wünnemann K, Collins GS, Melosh HJ. 2006. A strain-based porosity model for use in hydrocode simulations of impacts and implications for transient crater growth in porous targets. *Icarus* 180:514–27

Zahnle K, Schenk P, Levison H, Dones L. 2003. Cratering rates in the outer solar system. *Icarus* 163:263–89